This document is confidential and is proprietary to the American Chemical Society and its authors. Do not copy or disclose without written permission. If you have received this item in error, notify the sender and delete all copies.

Epoxy Resin-Encapsulated Polymer Microparticles for Room- Temperature Cold Sprayable Coatings

Journal:	ACS Applied Materials & Interfaces
Manuscript ID	am-2021-154155
Manuscript Type:	Article
Date Submitted by the Author:	12-Aug-2021
Complete List of Authors:	Huang, Mengfei; univeristy of Massachusetts Amherst, Chemical Engineering Liu, Yuan; University of Massachusetts Amherst, Chemical Engineering Khalkhali, Zahra; Manhattan College, Mechanical Engineering Kim, Ara; University of Massachusetts Amherst, Department of Mechanical and Industrial Engineering Hu, Weiguo; University of Massachusetts Amherst, Polymer Science and Engineering Lee, Jae-Hwang; University of Massachusetts Amherst College of Engineering, Mechanical & Industrial Engineering Rothstein, Jonathan; University of Massachusetts Amherst, Mechanical and Industrial Engineering Schiffman, Jessica; University of Massachusetts Amherst, Chemical Engineering

SCHOLARONE™ Manuscripts

Epoxy Resin-Encapsulated Polymer Microparticles for Room-Temperature Cold Sprayable Coatings

Mengfei Huang^{1,‡}, Yuan Liu^{1,‡}, Zahra Khalkhali², Ara Kim², Weiguo Hu³, Jae-Hwang Lee²,

Jonathan P. Rothstein², John Klier¹, Jessica D. Schiffman^{1,*}

- 1 Department of Chemical Engineering, University of Massachusetts Amherst, Amherst, MA 01003, United States
- 2 Department of Mechanical and Industrial Engineering, University of Massachusetts Amherst, Amherst, MA 01003, United States
- 3 Department of Polymer Science and Engineering, University of Massachusetts Amherst, MA 01003, United States
- [‡] These authors contribute equally.
- * Corresponding authors: Jessica D. Schiffman, Email: schiffman@ecs.umass.edu

ABSTRACT

We designed and synthesized epoxy-encapsulated microparticles with core-shell structures via suspension polymerization to enable high efficiency room-temperature cold spray processing. The soft core of the microparticles was comprised of a thermoset resin, diglycidyl ether of bisphenol A (DGEBA), which was optionally blended with the thermoplastic, poly(butyl acrylate); the protective shell was formed using polyurea. The composition, morphology, and thermo behavior of the microparticles were investigated. An inverse relationship between deposition efficiency and particle size was demonstrated by varying the surfactant concentration that was used during particle synthesis. We also determined that the

microparticles that had pure resin as the core had the lowest viscosity, a decrease in the critical impact velocity required for adhesion, the best flowability, and yielded a dramatic increase in deposition efficiency (56%). We have demonstrated that our in-house synthesized particles can form homogeneous, smooth, and fully coalesced coatings using room-temperature cold spray.

KEYWORDS: Coatings; Cold spray; Core-shell; Microencapsulation; Particles; Suspension polymerization

INTRODUCTION

Powder coatings are extensively used in industrial applications to provide superior performance, durability, and surface protection.¹⁻⁴ To form a coating, a thin layer of fine powder is deposited onto a substrate, followed by softening, fusion, and curing at an elevated temperature. In comparison with conventional solventborne coatings and aqueous polymer dispersions, powder coatings offer distinct economic and environmental advantages, including avoiding volatile organic compound (VOC) emissions, a reduced processing time, lower energy consumption during baking, and easy recycling of oversprayed powder.^{1,5-9} All of these advantages have prompted the development of highly competitive powder coatings in the coating market, however room for improvements remain.¹⁰

Various techniques have been developed to apply powder coatings, but they feature high temperatures to induce the powder to flow and cure. For example, when fluidized beds were used, the plates were preheated to 300-350 °C, dipped into the bed of fluidized powders for melting and film formation. ¹¹⁻¹² In the flame spray process, powders were introduced into the

flame of combusted fuel (in excess of 2900 K) via an inert carrier gas.¹³ Electrostatic spray utilizes electrical energy in the form of plasma or an arc to apply powders onto the metal substrate, but the deposition still requires baking in a hot-air oven with temperatures between 300-400 °C to consolidate the powders into a continuous coating.^{2, 5} While using electrostatic forces and high temperature baking significantly improves deposition efficiency and film formation, potential concerns remain. For example, the retention of the electrostatic charge decreases at higher temperatures and humidity levels, which restricts their use in outdoor applications. ¹⁴ Additionally, traditional thermal spray methods can result in undesired chemical reactions, high energy consumption and oxidation of compounds (e.g., aluminum, copper, organic). 13, 15 Heating powder coating requires ovens and precludes them from field applied maintenance applications commonly utilized to coat infrastructure (i.e., bridges, manufacturing facilities), ships, and other structures. Therefore, new methods are needed that enable the room-temperature application of powder coatings to eliminate the energy consumption and oxidation caused by high temperature baking, as well as to broaden their use in industrial and architectural applications.

Cold spray is a solid-state powder deposition process and an alternative to thermal spray methods. ¹⁶ Here, powders are accelerated in a de Laval nozzle with a stream of nitrogen, air, or helium gas at velocities ranging from 300 to 1200 m/s, while being sprayed onto a substrate that is held at a fixed standoff distance (nozzle exit to substrate distance). ¹⁷⁻¹⁹ Instead of thermal energy, kinetic energy typically forces particles to undergo plastic deformation on impact, therefore, high-temperature oxidation of powders could be avoided. ²⁰⁻²¹ Cold spray featuring metal particles (i.e., copper, aluminum, nickel, iron, zinc, tin, and alloys) has been extensively

investigated, whereas studies on the cold spray deposition of polymer particles are limited.²² Notably, polymer powders show limited deposition efficiency at room temperature; they require the assistance of electrostatic forces, substrate heating, or high impact velocities to achieve optimum adhesion. For example, when Xu et al. investigated the deposition of thermoplastic polyolefin powders onto a polyethylene substrate via room-temperature cold spray using a particle impact velocity of 130 m/s, less than 0.5% deposition efficiency was demonstrated and no deposition (0%) was observed on aluminum substrates.²³ Bush et al. conducted computational fluid dynamics simulations to optimize the design of nozzles where they determined the standoff distance that would improve deposition. However, the maximum deposition efficiency of the polyethylene particles was less than 3% at room temperature and reached 7.6% when the substrate temperature was heated to 120 °C.²¹ In addition to the commercially-available particles, polymeric microparticles with various chemistries and coreshell structures were designed and synthesized in-house in one cold spray investigation. Yang et al. successfully prepared novel poly(methyl methacrylate) (PMMA) particles containing epoxy resin diglycidyl ether of bisphenol A (DGEBA) as the thermosetting component. The deposition efficiency achieved was 10% at 160 °C and ~30% at 220 °C, however, no particle adherence was observed when the temperature of the aluminum substrate was below 160 °C (with compressed air at 206 kPa), thus limiting its use in industrial applications.²⁴ This was the first paper that evaluated deposition behavior in relation to particle chemistry, however, it was limited in scope. We suggest that new powders with lower glass transition temperatures (Tg) and softening points are need in order to achieve room-temperature cold spray processing with high deposition efficiency. Therefore, in this work, new particles are designed and synthesized

with a softer constructure to satisfy the criteria for room-temperature cold spray.

The suspension technique has been commonly used to prepare microcapsules that have a protective polymer shell and core substances for pharmaceuticals, enzymes, pigments, foods, and cosmetics. 25-28 In this work, we are interested in forming coatings using epoxy resins, which are reactive monomers that undergo crosslinking reactions with a variety of curing agents to form thermoset polymers that are widely used in high-performance coatings, adhesives, and electrical insulators due to their high modulus, durability and excellent chemical resistance. Most of the literature on epoxy-encapsulated microcapsules focuses on self-healing and toughening polymeric composites that use poly(urea-formaldehyde) as the shell. However, here we propose to use the microencapsulation technique to deliver epoxy resin within microparticles for use in additive manufacturing coating processes.

We designed a novel polymer powder coating system utilizing epoxy-encapsulated microcapsules to achieve room-temperature cold spray processing. The microparticles were synthesized via suspension polymerization, comprised of a thermoset resin core of diglycidyl ether of bisphenol A (DGEBA) optionally blended with thermoplastic poly(butyl acrylate) (PBA), and encapsulated within a polyurea (PU) shell, **Figure 1**. We designed these microparticles to test our hypothesis that a soft-core with a Tg below the processing/spraying temperature (which is room temperature in this work) is needed to achieve a high deposition efficiency and ultimately, to form a robust coating via room-temperature cold spray. We suggest that the core-shell structure could prevent agglomeration between microparticles, protect the reactive core components from reacting and leaking, enable an infinite shelf-life, and allow the on-demand curing of the powder coatings. In this work, the composition,

morphology and thermo behavior of in-house synthesized particles were investigated. The critical impact speed was screened using single particle impact experiments and the deposition efficiency was measured via cold spray. Notably, the use of pure-resin core in liquid state promoted the coalescence of epoxy to form films with a dramatically improved deposition efficiency compared to existing polymer powder coatings. This work explores several designs and chemical compositions of epoxy-encapsulated microparticles and provides a major advance towards the development of high-performance cold sprayable powder coatings with easy processibility and energy conservation.

MATERIALS AND METHODS

Materials. Bisphenol A diglycidyl ether (DGEBA), poly(vinyl alcohol) (PVA, molecular weight 13000-23000 Da, 87-89% hydrolyzed) and sodium dodecyl sulfate (SDS solution, 10 wt% in H₂O) were ordered from Sigma-Aldrich (St. Louis, MO). Butyl acrylate (BA, >99%, stabilized, Sigma-Aldrich) was used as monomer for the polymerization. Aluminum oxide (activated, basic, Brockmann I) and glass wool were obtained from Sigma-Aldrich and were used to remove the inhibitors from BA. Methylene di-p-phenyl diisocyanate (MDI, 98%, flakes, Sigma-Aldrich) and diethylenetriamine (DETA, 99%, polymer, Sigma-Aldrich) were used for shell formation. Methylene chloride (CH₂Cl₂, DCM, ≥ 99.5%) was used as the diluent agent purchased from Fisher Chemicals (Pittsburgh, PA). Epon 813, a low-viscosity (low-ŋ) liquid bisphenol-A based epoxy resin, was provided by Miller-Stephenson Inc. (Danbury, CT). Deionized (DI) water was used throughout the work.

Synthesis of Microparticles. Suspension polymerization was utilized for the synthesis of microparticles. The reactor comprised of a 1 L round-bottom four-neck reactor, a heating mantle, a mechanical stirrer for mixing and stirring rate control, a thermocouple for the accurate control of temperature and a nitrogen inlet to minimize the chain termination caused by oxygen. The schematic diagram for the synthesis of DGEBA-PBA-PU core-shell particle is shown in Figures 1 and S1(a). The dispersing solution was first prepared by dissolving PVA in DI water at 800 rpm and adding it to the 1 L reactor. SDS was added and mixed with PVA solution at 300 rpm under room temperature for 0.5 h. In the meantime, a monomer mixture was prepared by dispersing MDI, BA, DGEBA and AIBN into a homogeneous phase in a glass beaker before adding it into the reactor. The mixture was agitated at 300 rpm for 0.5 h under room temperature and N₂ environment. The strong shear stress caused by mechanical stirring led to the separation of hydrophobic monomers into small microdroplets, PVA and SDS were dispersed onto the surface of the droplets for stabilization. Each droplet acted as a single microreactor inside of which suspension polymerization occurred. Next, DETA was added and served as the shell reactant, the stirring rate was decreased to 150 rpm while the temperature was increased and kept at 60 °C for 1 h to complete the shell formation. Finally, the reactor temperature was increased to 80 °C for 3 h to completely polymerize the remaining BA. After the reaction, the particles were precipitated, washed with DI water three time to remove PVA and SDS, passed through the Buchner filter and dried in air overnight.

The synthesis procedure used to produce microparticles with incorporated DGEBA or an epoxy mixture with DGEBA and Epon 813 (low-ŋ epoxy) is shown in **Figure S1(b)** and the steps are similar to the synthesis of DGEBA-PBA-PU particles. The monomer mixture was

prepared by dispersing MDI, DGEBA with/without Epon 813 and DCM into a homogeneous phase in a glass beaker before adding it into the reactor. DCM was added to decrease the viscosity of the core and to facilitate the dispersion of the microdroplets. The mixture was agitated at 300 rpm for 0.5 h at room temperature and in an N₂ environment. DETA was then added and stirred at 150 rpm, 60 °C for 1 h to complete the formation of the polyurea shell. Meanwhile, DCM evaporated so that only DGEBA or the epoxy mixture remained inside the core. The formulations of microparticle synthesis with different core components are summarized in **Table 1**.

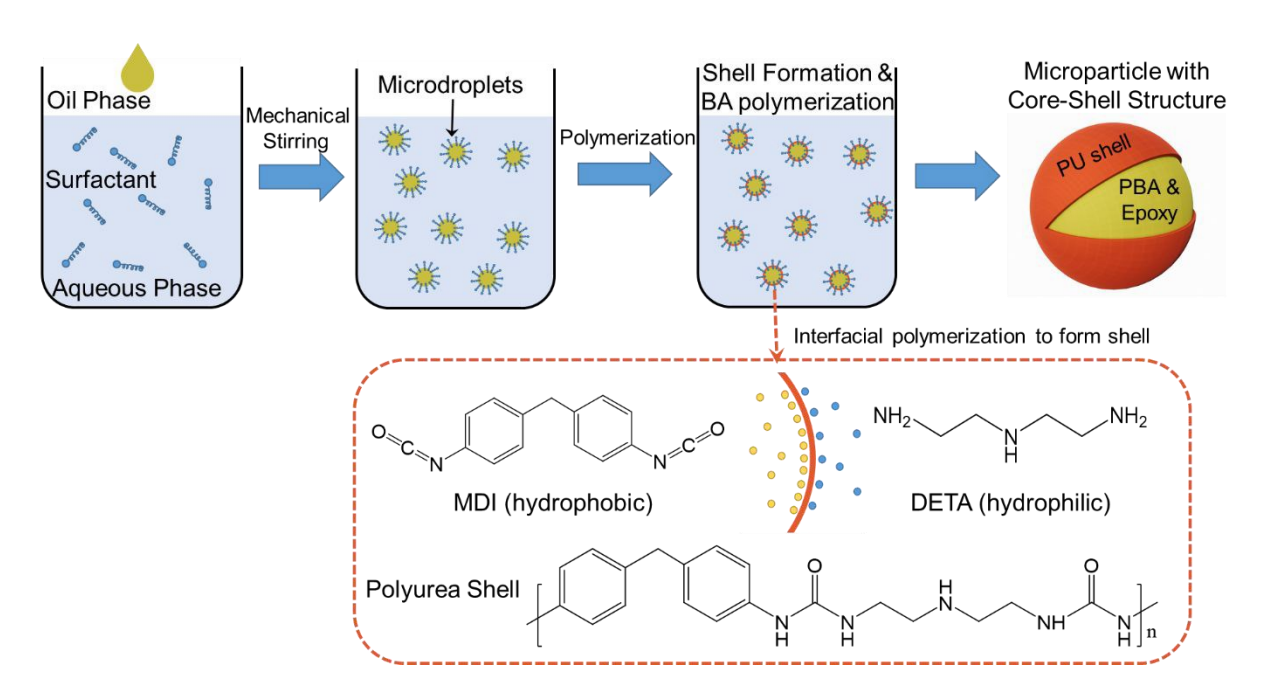


Figure 1. Schematic diagram of the suspension polymerization process used to synthesize DGEBA-PBA-PU core-shell particles. The reaction started with the formation of microdroplets upon mechanical stirring, followed by the interfacial polymerization between MDI and DETA to form a thin PU shell at 60 °C and the polymerization of BA into PBA. The temperature was further increased to 80 °C for the consumption of remaining monomers and finally resulted in a microparticle with core-shell structure. The schematic diagrams of synthesizing DGEBA-PBA-PU microparticle and DGEBA/Epoxy Mixture-PU microparticle are shown in **Figure S1**.

Table 1. Names and formulations of microparticles synthesized with different core components.

		Microparticle Name and Composition			
	Chemical (Unit)	DGEBA-PBA-PU	DGEBA-PU	Epoxy Mixture-PU	
Core	BA (g)	24	-	-	
	DGEBA (g)	40	40	20	
	Epon 813 (g)	-	-	20	
	DCM (g)	-	24	24	
	AIBN (g)	1.2	-	-	
Shell	MDI (g)	24	24	24	
	DETA (g)	10	10	10	
Dispersing agent	PVA (g)	16	16	16	
	SDS (g)	1.78	2.6	2.6	
	Water (g)	800	800	800	

Chemical Characterizations of Particles. The chemical composition of the particles was characterized using the solid-state nuclear magnetic resonance (ss-NMR, Bruker 600 MHz Avance III spectrometer), operating at a ¹H frequency of 600.13 MHz and ¹³C frequency of 150.90 MHz, in a 4 mm cross polarization/magic angle spinning (CP/MAS) probes. Several techniques were employed: (1) ¹H single-pulse experiments with 90° excitation, 2 dummy scans and 8 scans to estimate the ¹H T₁ relaxation time to be 1s for all samples. The spinning speed was 5 kHz. (2) CP/MAS experiments were conducted to qualitatively assess the rigid components. The pulse sequence was a 90° ¹H pulse followed by a CP period, then ¹³C detection with high-power ¹H decoupling. Recycle delay was 3 s and spinning speed was 5 – 8 kHz. (3) ¹³C DP (direct polarization)/MAS experiments. The recycle delay, decoupling field, and spinning speed were 60 s, 74 kHz, and 7 – 7.5 kHz, respectively.

Differential scanning calorimetry (DSC, Model Q200, TA Instruments) was conducted to determine the Tg of the polymer. The 3-5 mg polymer particle was weighed and added to a standard aluminum hermetic pan, which was sealed using TZERO press (TA Instruments)

before it was placed on the calorimeter. The equipment was equilibrated at 25 °C, heated to 200 °C using a temperature ramp of 10 °C/min, cooled to -70 °C and then heated again to 200 °C at the same rate. Thermogravimetric analysis (TGA, Q50, TA Instruments) was conducted to determine the degradation of microparticles. Polymer powders (7-10 mg) was loaded onto a platinum pan into the equipment and heated from 25 °C to 700 °C at a temperature ramp of 10 °C/min. The nitrogen was purged at a flow rate of 40 mL/min for the balance and 60 mL/min for the sample. The data was analyzed using Universal Analysis software (TA Instruments).

Characterization of Microparticles. The morphology of the microparticles and the particle deposition onto the galvanized steel substrates were observed using optical microscopy (ZEISS Microscope Axio Imager A2M) at 10X magnification. Scanning electron microscopy (SEM, FEI Magellan 400 XHR) was performed to characterize the surface morphology of the microparticles. Samples were coated with gold for 30s using a sputter coater (Cressington Scientific Instruments, Watford, UK) before imaging. Particle size distribution was imaged using a laser scanning confocal microscope (A1 series, Nikon Instruments Inc., Melville, NY) which was fitted with transmitted light detector of a 488 nm imaging laser, the data was analyzed using NIS Elements General Analysis.

Laser-Induced Single Microparticle Impact Experiments. The laser-induced projectile impact test (LIPIT) is an experimental method for assessing the dynamic responses of a material during high-strain-rate microscopic collisions and quantifying a critical velocity for bonding by visualizing the process of the impact.³⁴⁻³⁵ Polymeric microparticles were placed on top of the

elastomer layer (crosslinked polydimethylsiloxane, PDMS) of a launching pad consisting of three layers (PDMS/gold/glass), a single microparticle was accelerated by the ablation of a gold layer, which caused the rapid expansion of PDMS.³⁵ Microparticles with three different components including (1) DGEBA-PBA-PU, (2) DGEBA-PU and (3) Epoxy Mixture-PU were impacted onto an electropolished pure aluminum substrate. The acceleration of the microparticles was controlled at 350 m/s. The impact and rebound velocities were measured and calculated from stroboscopic micrographs taken by multiple ultrafast (<1ps) white light pulses with controlled time intervals.

Room Temperature Cold Spray Experiments. Cold spray was carried out using a home-built apparatus equipped with a compressed air inlet, an aluminum pressure vessel, a vibratory powder feeder, resistive heaters and a nozzle. Polymer powder having an initial mass in grams (m₁) was first loaded in the powder feeding hopper. The feeding of powder was accomplished by routing the carrier air around a vibratory powder dispenser (Pneumatic Vibrator VM-25, Cleveland Vibrator Co.). A rod connected the vibrator and pressure vessel, with a coarse wire mesh capped at the bottom, allowing the agitated powder to fall into the surrounding carrier gas. The gas pressure was monitored using a pressure transducer (PX309-300GV, Omega Engineering Inc.) and controlled at 90 psi, with an air speed at 370 m/s. The powder was sprayed onto the galvanized steel substrate at room temperature with a standoff distance of 15 mm. Any undeposited powder was collected and weighed (m₂). The initial weight of the galvanized steel substrate was taken as m₃ and weighed (m₄) after cold spraying. Thus, the deposition efficiency could be calculated via Equation 1.

Deposition Efficiency (%) =
$$\frac{m_4 - m_3}{m_1 - m_2} \times 100\%$$
 (**Equation 1**)

Viscosity Measurements. Microparticle cores chemistries with different formulations were prepared for viscosity measurements. DGEBA-PBA samples were prepared by mixing 40 g DGEBA with 24 g BA and 1.2 g AIBN in a 20 mL glass vial, then purged with N₂ for 10min and placed in the oven at 60 °C for 1 h and followed by 80°C for 3 h. Epoxy mixture was prepared by mixing DGEBA and low η epoxy at a 1:1 weight ratio at room temperature. Samples were placed onto the plate of the rheometer (AR2000 ETC, TA Instruments) for measurements using plastic pipettes. The test was conducted under constant frequency (6.283 rad/s) at 20.8 °C, the shear stress, strain and viscosity were determined.

RESULTS AND DISCUSSION

Characteristics of In-House Synthesized DGEBA-PBA-PU Microparticles

In this study, microparticles containing di-epoxy DGEBA as the reactive agent for room-temperature cold spray were synthesized via suspension polymerization, **Figure 1**. The microparticles were designed to have core-shell structures because we hypothesized that a shell could protect the soft-core components from agglomeration and allow for a longer shelf-life. The core featured PBA as the thermoplastic modifier and a softening agent along with the thermosetting component DGEBA. Based on our previous calculations and studies²⁴, the glass transition temperature (Tg) of the core structure needed to be lower than the processing temperature to achieve particles with excellent adhesion to a substrate and coalescence to form films. In our case, since the goal is room-temperature processing, we hypothesized that soft

particles might stick together upon reaction and after drying leading to difficulties in separating the particle aggregates, representing a significant challenge associated with processing them into coatings. To maintain free flowing particles, a PU shell was synthesized to protect the core structure, see **Figure 1**. The PU was formed based on the interfacial polymerization between the isocyanate groups of MDI and the amine groups of DETA, where the hydrophilic amine dissolved in the aqueous phase and reacted with isocyanate groups at the interface of the droplet. The reaction occurred rapidly at ambient temperature and could be accelerated at an elevated temperature. The resulting poly(MDI-DETA) chain precipitated and led to the formation of a protective shell around the droplet.³⁶ The morphology of the successfully synthesized spherical microparticles was characterized using optical microscope, as shown in **Figure 2(a)**. SEM was also used to image the surface of microparticles, and a smooth surface morphology was observed in **Figure 2(b)**. The following sections will detail the confirmation that the microparticles had a homogeneous size distribution (**Figure S2**) that was a function of surfactant concentration.

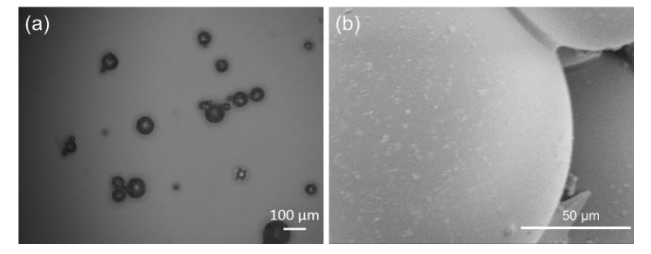


Figure 2. (a) Optical and (b) scanning electron micrographs of DGEBA-PBA-PU microparticles. Displayed are representative particles fabricated via suspension polymerization with BA: DGEBA: MDI: DETA = 24: 40: 24: 10 (weight ratio). The actual incorporation ratio of DGEBA in the particles was 41.7 wt% as determined using ss-NMR.

The core structure was comprised of a mixture of DGEBA and PBA. This was confirmed

using DSC; two Tgs, -18.1 °C and -38.0 °C, were displayed corresponding to the Tgs for DGEBA and PBA, respectively, **Figure S3**. The encapsulation of DGEBA was also demonstrated via TGA; the plot of the derivative weight versus temperature demonstrated that DGEBA degraded around 250 °C, and the peak for PBA was found at a higher temperature, above 320 °C, **Figure S4**. The encapsulation ratio of DGEBA into the particle was quantified to be 42.1 wt% via solid-state NMR, which was similar to the theoretical value (40.8 wt%), **Figure S5**. The slight variation could be explained by side emulsion polymerization of BA occurring in the aqueous phase, thus causing the PBA to decrease in the overall particle formulation (23.3 wt% versus the theoretical 34.7 wt% value).³⁷

Evaluation of the Critical Impact Velocity via Adherence of Single DGEBA-PBA-PU Microparticle to Aluminum Substrates

Single particle impact experiments were conducted using DGEBA-PBA-PU particles to investigate the deformation of the core-shell particles at a range of impact speeds, **Figure 3(a)**. In the impact experiment, single particles rebounded from the substrate for impact speeds below 308 m/s due to the elasticity of the PU shell. The rebound speed decreased when the impact speed was increased until a critical point was reached where the particle's shell was fractured upon impact and allowed the interior viscous DGEBA-PBA core to flow out and adhere to the surface. Therefore, particle's impact velocity exceeding the critical velocity is necessary for successful bonding and coating formation.

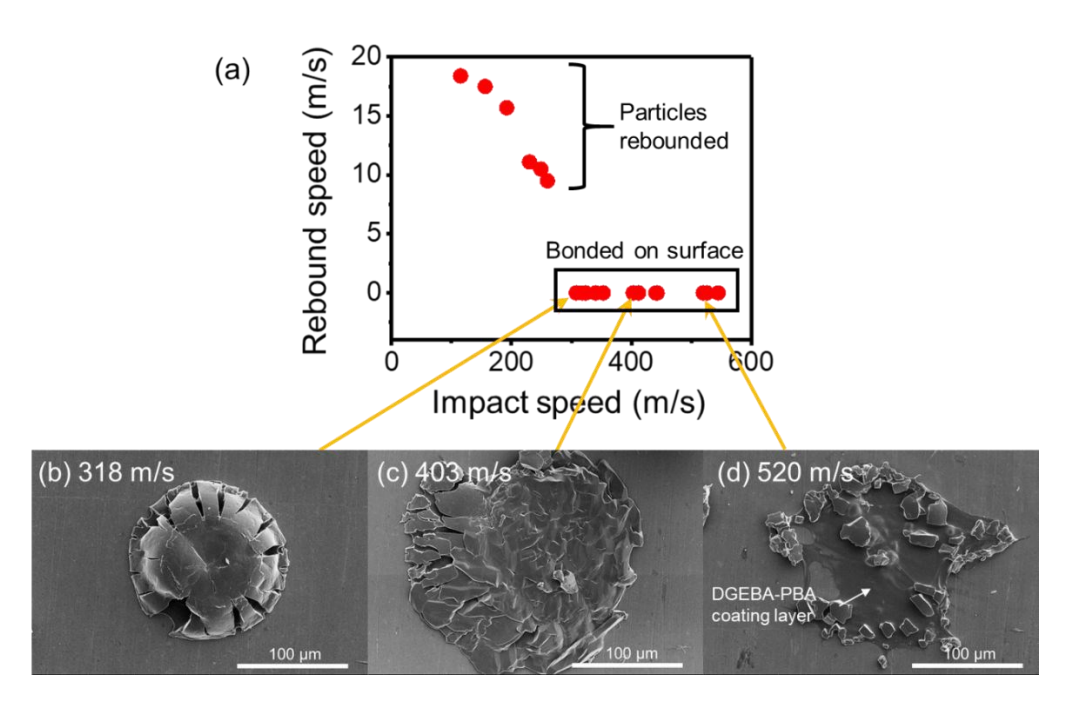


Figure 3. (a) Single particle impact experiments were conducted at room temperature via LIPIT to assess the dynamic responses of a particle during high-strain-rate microscopic collisions. The critical velocity needed for particle bonding onto an aluminum substrate was quantified. Representative DGEBA-PBA-PU particles with 42.1 wt% DGEBA encapsulation were tested. (b-d) Scanning electron micrographs of a particle after impacting the aluminum substrate at 318 m/s, 403 m/s and 520 m/s, respectively.

The deformation of the particles at the various impact velocities was observed using SEM. At an impact velocity of ~318 m/s, which was barely above the critical velocity, the radial fractures on the surface of particles were their most distinctive features, but the core of the particle remained inside, **Figure 3(b)**. The particle was completely fractured and laterally collapsed at an impact speed above 403 m/s, see **Figure 3(c)**. When the speed reached 520 m/s, the shell was shattered upon impact and the viscous core component was released and wet the impact surface, resulting in the formation of a homogeneous film coating on the aluminum substrate as shown in **Figure 3(d)**. Therefore, when the same composition and similar particle size (~100 µm) were tested, the degree of shell cracking and core release were highly dependent on the impact velocity, where excessively high impact velocity led to better film formation and

higher deposition efficiency. Thus, studying the critical velocity needed for optimal coalescence is essential for determining the minimum air speed needed during cold spray processing. The critical speed for a core-shell DGEBA-PBA-PU particle (with 42.1 wt% DGEBA encapsulation) to adhere onto the substrate without rebound was measured to be 308 m/s. It is worth noting that since excessively high impact velocity can cause significant material loss during the fracturing prosses (see **Figure 3(d)** for example), the optimal impact velocity should be determined through holistic consideration of fracture, mass loss, and wetting characteristics. LIPIT is a helpful tool in understanding the single particle impact behavior of a particle, but further optimizations might be needed when moving to the cold spray process.

Room-Temperature Cold Spray Deposition Efficiency as a Function of Surfactant Concentration and Particle Size

During the cold spray process, the size of the particles impacts their velocity when approaching the substrate. The drag force exerted on larger particles is larger than the force exerted onto smaller particles because of their lower surface to mass ratio, and subsequently, leading to lower force per unit mass. Therefore, larger particles accelerate more slowly resulting in lower impact velocities for the same pressure and nozzle configuration. Singh et al. concluded that the adhesion strength of cold sprayed metal particles was solely dependent on their kinetic energy at impact. We next explored how particle size impacted the deposition efficiency, keeping in mind that when we changed the particle size, the composition of the particles also changes slightly.

Our particles were synthesized using suspension polymerization, which involves

balancing droplet coalescence and droplet break-up during the vigorous mechanical stirring (Figure 1). Poly(vinyl alcohol) and/or surfactant are commonly used as stabilizers to enhance the stability of the droplets, prevent them from agglomeration, and controling the size distribution.³⁷⁻³⁸ In our study, SDS was chosen as a commonly used anionic surfactant to provide the electrostatic forces needed for droplet stabilization. Normally, SDS molecules will disperse on the surface of a droplet at an oil/water system, reduce the interfacial tension of the droplet and lead to smaller particle size on break-up. Particles were prepared at a series of SDS concentrations (from 0 to 1.5 CMC), with the same core components DGEBA:BA at a 24:40 weight ratio and shell of MDI:DETA at a 24:10 weight ratio. A mono dispersed particle size distribution was measured using a laser scanning confocal microscope, as shown in Figure S5. The particle size decreased when the amount of SDS was increased, from 275 µm to 101 µm when 0 CMC and 1 CMC were used, respectively. A plateau particle size of ~100 μm was observed when the SDS concentration was at or above 1 CMC, Figure 4(a). Therefore, SDS concentration at 1 CMC was regarded as the critical value where the maximum decrease of the droplet surface tension was achieved. Above 1 CMC, increasing the surfactant did not cause further changes to the particle size. Instead, surfactant molecules started to form micelles, which led to emulsion polymerization and miniemulsion polymerization as side reactions.³⁷ Therefore, controlling the surfactant concentration below 1 CMC was essential to stabilizing the reacting system and avoiding side reactions.

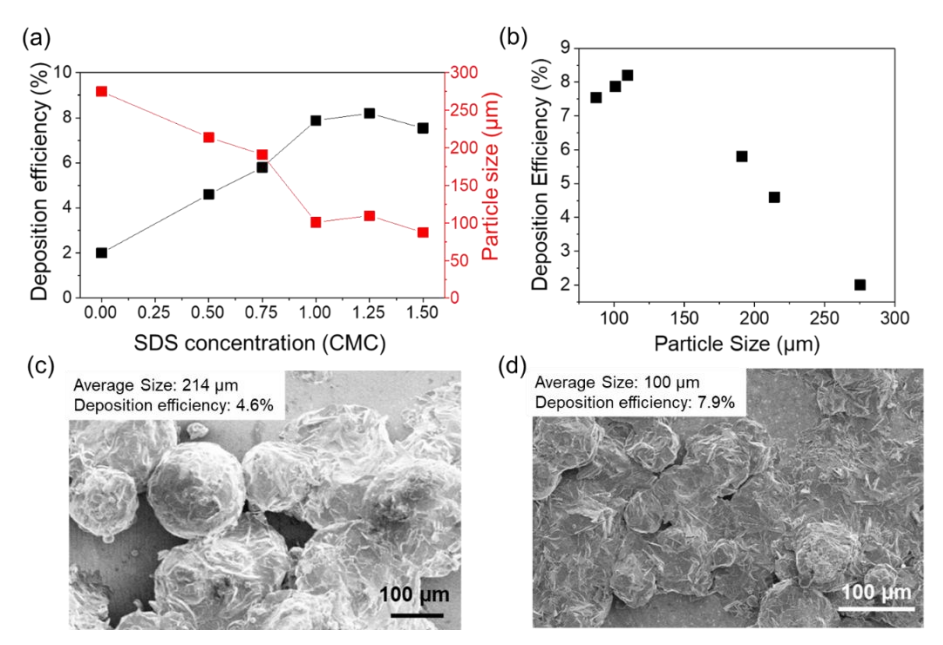


Figure 4. (a) DGEBA-PBA-PU microparticles were synthesized as a function of SDS concentration (from 0 to 1.5 CMC) via suspension polymerization. The deposition efficiency and particle size were evaluated as a function of the surfactant concentration. The critical micelle concentration (CMC) for SDS is 8.2 mM at 25 °C.³⁹ (b) The relationship between deposition efficiency and particle size. Scanning electron micrographs of cold sprayed particles synthesized with an average diameter of (c) 214 μ m and (d) 100 μ m. Particles were deposited onto galvanized steel at room temperature using an air pressure of 90 psi and an air speed of 370 m/s.

Air dried particles were sprayed onto galvanized steel using compressed air at room temperature to evaluate their deposition behavior. As displayed in **Figure 4(b)**, deposition efficiency was greater when the average particle size was smaller; there was a 2.0% deposition efficiency with 275 μm diameter particles vs. 7.9% with 100 μm particles. A maximum deposition efficiency plateau of 8.2% was achieved when the particles were synthesized using 1.25 CMC. This could be explained by the higher spraying speed generated from smaller particles under the same kinetic energy provided by gas jet, while larger particles take longer to accelerate. The impact of the microparticles onto the substrate causes the PU shell to break and subsequently, the soft DGEBA-PBA core is released from the particles onto the substrate and coalescences to form a film. The surface morphology of particles deposited via cold spray

are provided in Figure 4(c)(d). The larger particles that had an average size of 214 µm maintained their spherical shape upon impact, whereas smaller particles with average size of 100 µm shattered on the substrate and achieved better coalescence and film formation. Therefore, the size of polymer particles is an important factor considering the improvement of deposition efficiency from the application standpoint, which could be optimized by using different polymer chemistries, synthesis formulations and mixing conditions, etc. We acknowledge that fabricating much smaller particles via our current chemistry and suspension polymerization would be challenging because further increasing of surfactant concentration (above 1 CMC) would result in emulsion polymerization side reactions, and the incorporation of a shell structure would enlarge the overall microparticle size. On the other hand, if the particles are too small, they would not impact the substrate, but instead they would follow the flow streamlines away from the surface. As a result, there does exist a lower limit for the diameter of particles for our in-house constructed cold spray configuration, which is ~2 μm (calculations available upon request).

Design of Microparticles with Different Core Formulations

Particle core composition was studied to determine its influence on cold spray deposition efficiency. The Tg and viscosity of particles with three different core chemistries are provided in **Table 2**. The viscosity of pure DGEBA and the epoxy mixture were 48 Pa.s and 21 Pa.s, respectively, which were much lower than DGEBA-PBA (2500 Pa.s). During the synthesis of DGEBA-PBA-PU microparticles, BA monomer acts as a diluent for DGEBA to reduce the viscosity of the oil phase for better dispersion, encapsulation of the core, and improved particle

size distribution. Upon heating, the thermal initiator AIBN dissociates into free radicals and initiates BA to polymerize into long chain PBA, leading to a significant increase in the core viscosity. Even though the PBA component was soft enough (Tg of -39 °C), we hypothesize that due to its contribution to an overall higher viscosity of the core (2500 Pa.s), it was not able to sufficiently deform and coalescence into a homogeneous coating. This explained the relatively poor film formation performance of DGEBA-PBA-PU microparticles as previously discussed in **Figure 4(c)(d)**, and the resulting low deposition efficiency of 8% via room-temperature cold spray. In comparison, liquid-state DGEBA and the epoxy mixture were better core candidates because they exhibited improved flowability due to their lower viscosity and could directly flow out of the shell upon impact to form a film.

Table 2. Formula and physical properties of particles prepared with different core compositions.

	Particle Core Composition		
			Epoxy Mixture
	DGEBA-PBA	DGEBA	(W _{DGEBA} : W _{Epon 813} = 1:1)
Core Tg (°C)†	-38.0, -18.1	-19.1	-30.6
Core Viscosity (Pa.s)‡	2500	48	21
Deposition efficiency			
(%)^	8	28	56
Epoxy output (wt%)*	41.7	66.5	58.4

[†]Determined using differential scanning calorimetry

To further improve the deposition behavior of microparticles, we investigated two other core formulations, low-n liquid bisphenol-A based epoxy resin (Epon 813) and DCM as the substitutes for BA. During the synthesis, DCM evaporated at an elevated temperature, leaving

[‡]Determined using rheology

[^]Determined using room-temperature cold spray experiments

^{*}Measured using solid-state NMR

only DGEBA or epoxy mixture (DGEBA and Epon 813) inside the particle's core. Therefore, the microparticles exhibited a core-shell structure with a liquid core formulation. The incorporation ratio of DGEBA and epoxy mixture was quantified via solid-state NMR to be 66.5 wt% and 58.4 wt%, respectively, which were both were higher than DGEBA-PBA (41.7 wt%) as the core, **Figure S7**. Notably, only one Tg was displayed for the microparticles that had the epoxy mixture as the core as displayed in **Figure S6(e)**, which suggests that there was a homogeneous dispersing and mixing between DGEBA and Epon 813. Additionally, the encapsulation of epoxy was verified via TGA experiments, where the degradation peaks of DGEBA and Epon 813 were confirmed to be at 260 °C and 142 °C, respectively, **Figure S8**.

Room-Temperature Cold Spray Deposition Efficiency and Critical Velocity as a Function of Particle Core Composition

The deposition efficiency substantially increased to 28% for particles with DGEBA as the core and to 56% with epoxy mixture as the core. The inverse correlation between viscosity and deposition efficiency are illustrated in **Figure 5(a)**. The resulting homogeneous, smooth, and fully coalesced film deposited using particles encapsulated with the epoxy mixture is displayed in **Figure 5(b)**. This is a breakthrough compared with the existing powder coating systems established for room-temperature cold spray. Therefore, the incorporation of liquid core structure significantly enhanced the film formation performance, as well as improved the loading capability of reactive epoxy.

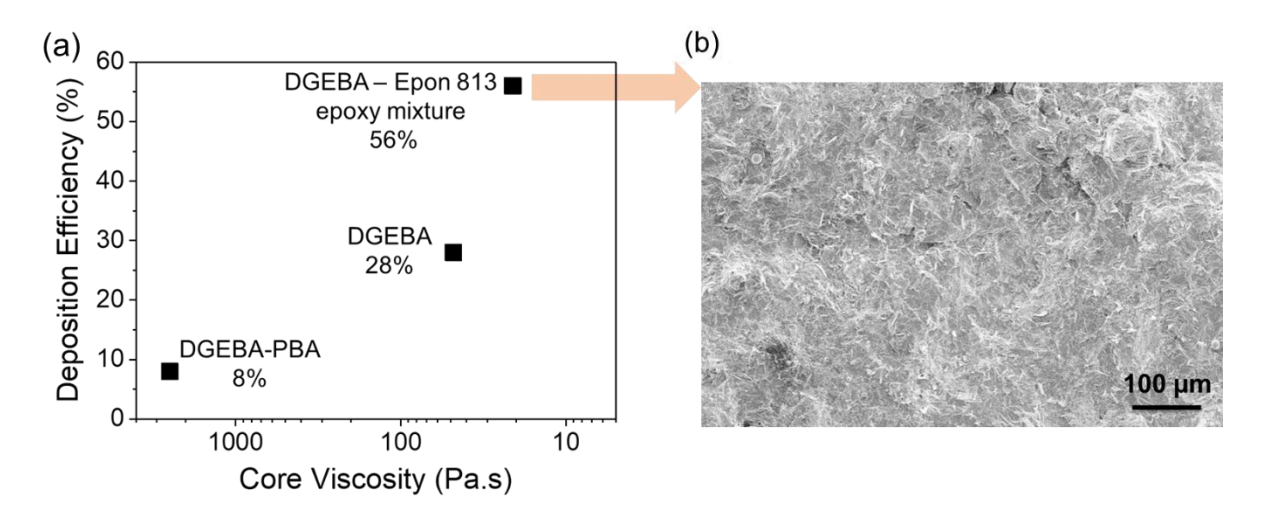


Figure 5. (a) Particle deposition efficiency as a function of the viscosity of the particle's core components, including DGEBA-PBA, DGEBA and epoxy mixture. Viscosity measurements were conducted using rheology. (b) Optical micrograph of the fully coalesced Epoxy Mixture-PU particle coating formed via room temperature cold spray onto galvanized steel using an air pressure of 90 psi and an air speed of 370 m/s.

The critical particle velocity needed to form cold sprayed coatings was next determined using particles that had an (1) epoxy mixture as the core and (2) DGEBA-PBA as the core. These results were compared to the published work by Yang et al. using DGEBA-PMMA particles (no shell structure).²⁴ Since PMMA has a Tg of 105 °C, the optimized DGEBA-PMMA core still remained a solid at the spraying temperature (room temperature), and required a higher speed to bond on the substrate. Yang et al. suggested that the particles exhibited good film formation using electrostatic spraying with a heated substrate (above 200 °C); the deposition efficiency was less than 3% via room-temperature cold spray. However, by introducing only the epoxy mixture as the core and leveraging the protective core-shell structure, the core viscosity tremendously decreased which further facilitated the adherence of particles onto the substrate. The critical velocity decreased as the core viscosity decreased, as shown in Figure 6, from 308 m/s for the DGEBA-PBA to 173 m/s for the epoxy mixture, and

both of the particles required a much lower critical velocity compared to the DGEBA-PMMA particles (438 m/s).²⁴ Therefore, our reactive particles developed with a liquid core demonstrated a dramatic improvement in both film formation and the deposition efficiency via room-temperature cold spray, as well as a reduced impact velocity needed for application, without heating or electrostatic forces, which provides a significant step forward for the development of industrial powder coatings.

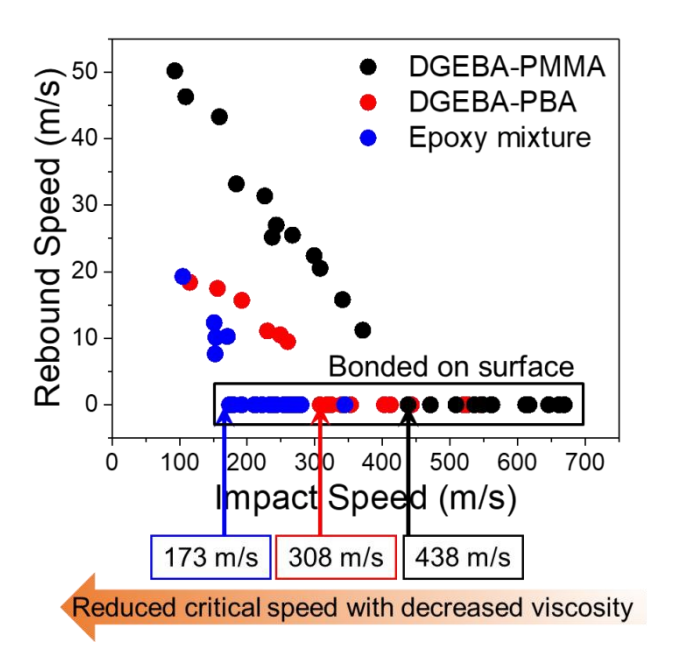


Figure 6. Rebound speed versus impact speed of DGEBA-PMMA (12:20, no shell, black symbols), DGEBA-PBA-PU (40:24, core-shell, red symbols) and Epoxy Mixture-PU (20:20, core-shell, blue symbols) particles determined using single particle impact experiments at room temperature. The size of all particles was $\sim 100 \ \mu m$.

CONCLUSION

In summary, epoxy resin-encapsulated polymer microparticles were designed and synthesized via suspension polymerization for room-temperature cold spray. The particle, with a core-shell structure, is comprised of a soft-core of thermoset resin DGEBA modified with thermoplastic PBA and a protective PU shell. The particle's surface morphology was

determined to be spherical and smooth by optical and scanning electron microscopy. The encapsulation of DGEBA was demonstrated by the appearance of two distinct Tgs in the core as measured via DSC whereas the DGEBA degradation peak was found via TGA, and the encapsulation ratio was calculated directly via ss-NMR spectra to be 42.1 wt%. The critical impact velocity of DGEBA-PBA-PU particle was investigated using LIPIT, where the adherence of a particle on an aluminum substrate occurred when the impact velocity was above 308 m/s. Microparticle size decreased with the increasing surfactant concentration, and the particle size was inversely related to the cold spray deposition efficiency due to the higher impact velocity generated for smaller particles. Furthermore, particles with different core chemistries and viscosities were evaluated in affecting the deposition efficiency and the critical impact velocity. Particles that had a liquid core with only DGEBA or an epoxy mixture (DGEBA and Epon 813) were demonstrated to have a dramatic improvement in both film formation and deposition efficiency, up to 56%, when compared to the typical cold spray deposition efficiencies of less than 10%. Our work represents a significant breakthrough and path towards achieving reliable, efficient cold spray coatings at room temperature.

Supporting information. Schematic diagrams of particle synthesis procedures, DSC and TGA diagrams, ss-NMR spectra, particle size distribution diagrams are provided.

AUTHOR INFORMATION

Corresponding Authors

*Emails: schiffman@ecs.umass.edu (J.D.S.)

Notes: The authors declare no competing financial interest.

ACKNOWLEDGEMENTS. The authors thank Dr. Guozhen Yang for the preliminary experiments and insightful conversations. M.H. was supported by National Research Service Award T32 GM008515 from the National Institutes of Health. The authors acknowledge the financial support from U.S. Army Research Laboratory (ARL W911NF-15-0024 and NCMS 202028-141054). A.K. and J.-H.L acknowledge the support of the National Science Foundation (CMMI-1760924).

REFERENCES

- (1) Barletta, M.; Lusvarghi, L.; Mantini, F. P.; Rubino, G., Epoxy-based thermosetting powder coatings: Surface appearance, scratch adhesion and wear resistance. *Surf. Coat. Technol.* **2007**, *201* (16-17), 7479-7504.
- (2) Morancho, J.; Salla, J.; Ramis, X.; Cadenato, A., Comparative study of the degradation kinetics of three powder thermoset coatings. *Thermochim Acta* **2004**, *419* (1-2), 181-187.
- (3) Sharifi, M.; Ebrahimi, M.; Jafarifard, S., Preparation and characterization of a high performance powder coating based on epoxy/clay nanocomposite. *Progress in Organic Coatings* **2017**, *106*, 69-76.
- (4) Huang, M.; Yang, G.; Klier, J.; Schiffman, J.; Palsule, A.; Holzer, M. R., Emulsion polymers crosslinked with compounds containing two or more dicarbonyl-substituted 1 alkene units. US Patent App. 16/957,763: 2021.

- (5) Meng, X.; Zhang, H.; Zhu, J. J., Characterization of particle size evolution of the deposited layer during electrostatic powder coating processes. *Powder Technol* **2009**, *195* (3), 264-270.
- (6) Pearnchob, N.; Bodmeier, R., Dry polymer powder coating and comparison with conventional liquid-based coatings for Eudragit® RS, ethylcellulose and shellac. *Eur J Pharm Biopharm* **2003**, *56* (3), 363-369.
- (7) Andrei, D.; Hay, J.; Keddie, J.; Sear, R.; Yeates, S., Surface levelling of thermosetting powder coatings: theory and experiment. *J. Phys. D: Appl. Phys.* **2000**, *33* (16), 1975.
- (8) Bailey, A. G., The science and technology of electrostatic powder spraying, transport and coating. *J Electrostat* **1998**, *45* (2), 85-120.
- (9) Huang, M.; Liu, Y.; Yang, G.; Klier, J.; Schiffman, J. D., Anionic Polymerization of Methylene Malonate for High Performance Coatings. *ACS Applied Polymer Materials* **2019**. (10)Lee, S. S.; Han, H. Z.; Hilborn, J. G.; Månson, J.-A. E., Surface structure build-up in thermosetting powder coatings during curing. *Progress in organic coatings* **1999**, *36* (1-2), 79-88.
- (11)Takeshita, Y.; Kamisho, T.; Sakata, S.; Sawada, T.; Watanuki, Y.; Nishio, R.; Ueda, T., Dual layer structural thermoplastic polyester powder coating film and its weathering resistance. *Journal of applied polymer science* **2013**, *128* (3), 1732-1739.
- (12)Barletta, M.; Gisario, A.; Guarino, S.; Rubino, G., Development of smooth finishes in electrostatic fluidized bed (EFB) coating process of high-performance thermoplastic powders (PPA 571 H). *Progress in organic coatings* **2006**, *57* (4), 337-347.
- (13)Ang, A. S. M.; Berndt, C. C., A review of testing methods for thermal spray coatings. *Int Mater Rev* **2014**, *59* (4), 179-223.

- (14)Xu, Y.; Barringer, S., Effect of relative humidity on coating efficiency in nonelectrostatic and electrostatic coating. *J Food Sci* **2008**, *73* (6), E297-E303.
- (15)Karthikeyan, J., The advantages and disadvantages of the cold spray coating process. In *The cold spray materials deposition process*, Elsevier: 2007; pp 62-71.
- (16)Rokni, M.; Nutt, S.; Widener, C.; Champagne, V.; Hrabe, R., Review of relationship between particle deformation, coating microstructure, and properties in high-pressure cold spray. *J Therm Spray Techn* **2017**, *26* (6), 1308-1355.
- (17)Singh, H.; Sidhu, T.; Kalsi, S., Cold spray technology: future of coating deposition processes. *Frattura ed Integrità Strutturale* **2012**, *6* (22), 69-84.
- (18)Stenson, C.; McDonnell, K.; Yin, S.; Aldwell, B.; Meyer, M.; Dowling, D.; Lupoi, R., Cold spray deposition to prevent fouling of polymer surfaces. *Surf. Eng.* **2018**, *34* (3), 193-204. (19)Assadi, H.; Kreye, H.; Gärtner, F.; Klassen, T., Cold spraying–A materials perspective. *Acta Mater* **2016**, *116*, 382-407.
- (20)Moridi, A.; Hassani-Gangaraj, S. M.; Guagliano, M.; Dao, M., Cold spray coating: review of material systems and future perspectives. *Surf. Eng.* **2014**, *30* (6), 369-395.
- (21)Bush, T. P.; Khalkhali, Z.; Champagne, V.; Schmidt, D. P.; Rothstein, J. P., Optimization of cold spray deposition of high-density polyethylene powders. *J Therm Spray Techn* **2017**, *26* (7), 1548-1564.
- (22)Khalkhali, Z.; Xie, W.; Champagne, V. K.; Lee, J.-H.; Rothstein, J. P., A comparison of cold spray technique to single particle micro-ballistic impacts for the deposition of polymer particles on polymer substrates. *Surf. Coat. Technol.* **2018**, *351*, 99-107.
- (23)Xu, Y.; Hutchings, I., Cold spray deposition of thermoplastic powder. Surf. Coat. Technol.

2006, *201* (6), 3044-3050.

- (24)Yang, G.; Xie, W.; Huang, M.; Champagne, V. K.; Lee, J.-H.; Klier, J.; Schiffman, J. D., Polymer Particles with a Low Glass Transition Temperature Containing Thermoset Resin Enable Powder Coatings at Room Temperature. *Industrial & engineering chemistry research* **2018**, *58* (2), 908-916.
- (25)Gouin, S., Microencapsulation: industrial appraisal of existing technologies and trends. *Trends Food Sci Tech* **2004**, *15* (7-8), 330-347.
- (26)Jacquemond, M.; Jeckelmann, N.; Ouali, L.; Haefliger, O. P., Perfume-containing polyurea microcapsules with undetectable levels of free isocyanates. *Journal of applied polymer science* **2009**, *114* (5), 3074-3080.
- (27)Dubey, R., Microencapsulation technology and applications. *Defence Sci J* **2009**, *59* (1), 82.
- (28)Huang, M.; Liu, Y.; Klier, J.; Schiffman, J. D., High-Performance, UV-Curable Crosslinked Films via Grafting of Hydroxyethyl Methacrylate Methylene Malonate. *Industrial & Engineering Chemistry Research* **2020**.
- (29)Yuan, L.; Gu, A.; Liang, G., Preparation and properties of poly (urea-formaldehyde) microcapsules filled with epoxy resins. *Mater Chem Phys* **2008**, *110* (2-3), 417-425.
- (30)Yuan, L.; Liang, G.; Xie, J.; Li, L.; Guo, J., Preparation and characterization of poly (ureaformaldehyde) microcapsules filled with epoxy resins. *polymer* **2006**, *47* (15), 5338-5349.
- (31)Jin, H.; Mangun, C. L.; Stradley, D. S.; Moore, J. S.; Sottos, N. R.; White, S. R., Selfhealing thermoset using encapsulated epoxy-amine healing chemistry. *Polymer* **2012**, *53* (2), 581-587.

- (32)Liu, X.; Zhang, H.; Wang, J.; Wang, Z.; Wang, S., Preparation of epoxy microcapsule based self-healing coatings and their behavior. *Surf. Coat. Technol.* **2012**, *206* (23), 4976-4980. (33)Jin, H.; Mangun, C. L.; Griffin, A. S.; Moore, J. S.; Sottos, N. R.; White, S. R., Thermally stable autonomic healing in epoxy using a dual-microcapsule system. *Adv Mater* **2014**, *26* (2), 282-287.
- (34)Lee, J.-H.; Loya, P. E.; Lou, J.; Thomas, E. L., Dynamic mechanical behavior of multilayer graphene via supersonic projectile penetration. *Science* **2014**, *346* (6213), 1092-1096.
- (35)Lee, J.-H.; Veysset, D.; Singer, J. P.; Retsch, M.; Saini, G.; Pezeril, T.; Nelson, K. A.; Thomas, E. L., High strain rate deformation of layered nanocomposites. *Nature communications* **2012**, *3* (1), 1-9.
- (36)Cho, J.-S.; Kwon, A.; Cho, C.-G., Microencapsulation of octadecane as a phase-change material by interfacial polymerization in an emulsion system. *Colloid and polymer science* **2002**, *280* (3), 260-266.
- (37)Dowding, P. J.; Vincent, B., Suspension polymerisation to form polymer beads. *Colloids and Surfaces A: Physicochemical and Engineering Aspects* **2000**, *161* (2), 259-269.
- (38)Ramirez, J. C.; Herrera-Ordonez, J.; Gonzalez, V. A., Kinetics of styrene minisuspension polymerization using a mixture PVA–SDS as stabilizer. *Polymer* **2006**, *47* (10), 3336-3343.
- (39)Miura, M.; Kodama, M., The second CMC of the aqueous solution of sodium dodecyl sulfate. I. Conductivity. *B Chem Soc Jpn* **1972**, *45* (2), 428-431.

TOC FIGURE

